METHODOLOGY FOR AUTOMOTIVE AIR-CONDITIONING CONTROL OPTIMIZATION USING ARTIFICIAL NEURAL NETWORKS

R. P. Mendes[a],
K. Cancado[a],
L. V. S. Martins[a],
J. J. G. Pabon[a],
and L. Machado[a]

[a]Universidade Federal de Minas Gerais
Programa de Pós-graduação em Engenharia Mecânica
Av. Antônio Carlos, 6627
CEP. 31270-901, Belo Horizonte, Minas Gerais, Brasil
Belo Horizonte, Minas Gerais, Brasil
ramondepaoli@yahoo.com.br
kancado@hotmail.com
leo.vsm@hotmail.com
jjgp@unifei.edu.br
luizm@demec.ufmg.br

Received: Dec 06, 2021
Revised: Dec 28, 2021
Accepted: Dec 30, 2021

ABSTRACT

The transient nature of automotive air conditioning systems control is generally achieved through proportional–integral–derivative controllers (PID's) parameters tunning. Due to the vast database available from decades of automotive manufacturers design and expertise, Artificial Neural Networks (ANN) might be able to identify underlying patterns to predict and properly tune the air-conditioning PID control systems under different thermal requirements. Recently, advances in computational capability have enabled compact embarked systems to rapidly solve complex, multi-variable sets of equations, thus allowing for ANN to promptly calculate tunning parameters and act upon PID controllers. As any new application, technical literature is still scarce. On this research, a coupled PID and 6-layers perceptron ANN system was devised, programmed and used to simulate how an air-conditioning system performance can be optimized through proportional–integral–derivative controllers tuning. This proposed setup response was then compared to a conventional heuristic PID tunning method (Ziegler Nichols) to demonstrate how ANN's can more rapidly stabilize the system output.

Keywords: heat optimization; artificial neural networks; PID; air-conditioning.

NOMENCLATURE

c	specific heat, kJ/(kg.K)
E	error
K	controller gain
m	mass, kg
$\dot{m}$	mass flow, kg/s
Q	thermal load, kW
T	temperature

Greek Symbols

β	sigmoidal function constant
η	network learning rate
δ	network gradient
θ	network activation limit

Acronyms

ANN	Artificial Neural Network
GWP	Global Warming Potential
VC	Controlled Variable

Subscripts

0	initial
air	air
amb	environmental
cab	cabine
d	derivative
dif	difuse
dir	direct
eng	engine
eva	evaporation
exa	exhaust
met	metabolic
fluid	cooling fluid
i	entrance
I	integrative
p	proportional
ref	reflected
ven	ventilation

INTRODUCTION

Diminishing carbon emissions worldwide is a crucial outstanding challenge in our species survival. Back in 1997, the Kyoto Protocol was agreed upon by UN member nations setting ambitious, albeit necessary environmental goals (Hassan, 2013). To abide to these requirements, the European Union decided to outlaw, from 2017 onwards, refrigerant fluids with Global Warming Potential (GWP) greater than 150 CO_2eq in automotive applications, and 750 CO_2eq on stationary units (European Commission, 2006). This policy, which is likely to be emulated by other nations, lead to research and development of new refrigerant alternatives capable of meeting the performance requirements whilst mitigating, or avoiding altogether, environmental impact. However, these new, low-impact fluids are unable to reach the same level of performance of the conventional refrigerants, with heat transfer coefficient around 20% below their older alternatives (Yang and Nalbandian, 2018). So being, effective control techniques become paramount in guaranteeing their widespread adoption, especially in compact and portable automotive units. Specifically, to the motor vehicle scenario, effectively controlling the air temperature inside the passenger's compartment can reduce fuel consumption and increases the overall thermal comfort. Usually, the air temperature in the main passenger compartment is measured, and used as feedback to the control system, which tunes the proportional, integrative and/or proportional gains in a PID controller, whose operation follows the equation (Ogata, 2001):

$$VC = K_p \cdot E + K_I \cdot \int_0^t E \cdot dt + K_p \cdot K_d \cdot \frac{dE}{dt} \cdot \cdot S_0 \qquad (1)$$

Where VC is the variable to be controlled, K_p, K_I and K_d are the PID proportional, integrative and derivative gains, respectively, E corresponds to the error from a reference value, S_0 is the PID initial output and t is the time component. The three gain variables are adjusted in accordance to the system requirements, being able to completely alter how a controlled air conditioning installation operates and performs. Albeit slow, conventional tuning methods like Ziegler Nichols (Ogata, 2001), Chien-Hrones-Reswick (Sen et al., 2014) and Fuzzy logic (Visioli, 2001) are able to properly define K_p, K_I and K_d values to meet a thermal comfort demand. More recently, Artificial Neural Networks (ANN) techniques have been proposed as a replacement for these conventional approaches, as they can solve virtually any problem, given enough time and training. An ANN operates similarly to a biological neuron network, wherein chemicals concentrations are adjusted to better respond to a given outside stimulus. Similarly, in an artificial neural network a set of synaptic weights is assigned to neural nodes, whose values are adjusted depending on input information and output requirements, in a process called supervised learning (Nunes et al., 2010).

In the automotive industry, ANN have been proposed and implemented in recently published studies. Zhang et al. (2020) proposed using ANN to improve the positioning response obtained from satnav signals. By implementing a fuzzy logic to an artificial neural network system, higher positioning accuracy was achieved faster than the conventional triangulation method, skipping unnecessary intermediate calculations. Nie et al. (2018) compared the response quality of PID control over a car cruise velocity by implementing a fuzzy logic with and without integration with an ANN, showing how the latter performance was superior to a standalone fuzzy logic.

The dynamic nature of automotive vehicles, wherein several non-modelled disturbances, variable external conditions, different loads, geometries and requirements influence a given controlled variable result in classical PID tuning methods performing at various levels of performance. Under these diverse set of requirements, each of the controller gains must be set accordingly, and ANN are particularly fit to accomplish it. The main goal of the present work is to study the interactions between an automotive air conditioning PID and an ANN controlling it, ultimately investigating the agility of tunning, fuel consumption reduction and the improvement on the overall cycle COP.

The next chapter will consist of the automotive AC thermal model description, followed by the PID controller main equations and the ANN developed for this application. In the Simulation section, the main methodology used in the current paper will be presented, lastly followed by the results and the corresponding discussion and conclusions.

THERMAL MODELLING

The first step to develop a thermal model consists of defining the relevant loads entering and leaving the studied control volume, how they interact and the desired resulting state. In this sense, the thermal loads to be considered entering the control volume (passenger compartment) are incoming thermal radiation (both diffuse and direct incidence), net convective heat transfer with the surroundings, thermal energy incoming from the engine compartment and exhaustion systems and heat released from the passengers inside the car. This thermal load is balanced by the air conditioning must remove heat energy from the air mass inside the passenger compartment, as proposed and detailed by Khayyam et al. (2009). In Fig. 1 the thermal interactions are described.

Considering a constant air mass inside the passenger compartment, its temperature change is defined by the net thermal load balance:

$$m_{air} \cdot c_p \cdot \frac{dT}{dt} = \dot{Q}_{net} \tag{2}$$

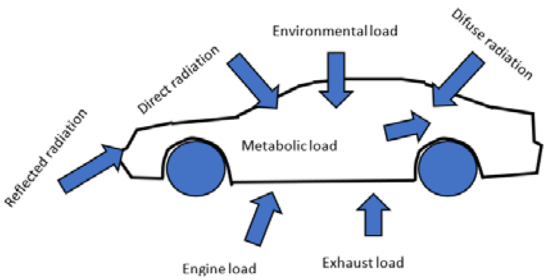

Figure 1. Thermal incidence on the vehicle.

Where m_{air} is the air mass in kg, c_p is the constant pressure specific heat ($Jkg^{-1}K^{-1}$), $\dot{Q}_{net}$ is the net sum of heat flow rates into – and out of the control volume in watts and, finally, $\frac{dT}{dt}$ is the rate of air temperature change, in K/s. The net heat flow rate can be broken down into its constituents, which will be used to design and size the AC system evaporator unit.

$$\dot{Q}_{net} = \begin{array}{l} \dot{Q}_{met} + \dot{Q}_{dir} + \dot{Q}_{dif} + \dot{Q}_{ref} + \dot{Q}_{amb} \\ +\dot{Q}_{exa} + \dot{Q}_{eng} + \dot{Q}_{ven} - \dot{Q}_{eva} \end{array} \tag{3}$$

Under steady state conditions, the net temperature change over time is defined to equalise zero. Moreover, according to Fayazbakhsh and Fayazbakhsh (2013) the thermal loads incoming the engine bay, exhaustion system and reflected off the ground can be neglected. So, Eq. (3) can be rewritten as

$$\dot{Q}_{eva} = \dot{Q}_{met} + \dot{Q}_{dir} + \dot{Q}_{dif} + \dot{Q}_{amb} + \dot{Q}_{ven} \tag{4}$$

Applying the energy balance equation to the refrigerant fluid flowing in the refrigeration system:

$$\begin{array}{l} \dot{m}_{fluid} \cdot c_{p,fluid} \cdot (T_{in} - T_{out}) = \\ \dot{Q}_{met} + \dot{Q}_{dir} + \dot{Q}_{dif} + \dot{Q}_{amb} + \dot{Q}_{ven} = \dot{Q}_{net} \end{array} \tag{5}$$

Algebraic manipulation of the previous equations exposes the linear dependence between the net refrigeration load ($\dot{Q}_{net}$) and the refrigerant mass flow rate ($\dot{m}_{fluid}$) and inversely proportional to the thermal incline ($c_{p,fluid}\Delta T_{evap}$):

$$\dot{m}_{air} = \frac{\dot{Q}_{net}}{c_{p,fluid} \cdot (T_{in} - T_{out})} \tag{6}$$

PID CONTROLLERS

A number of different process control techniques are currently applied in the industry. Within these, PID control is one of the mainstream ongoing industry standards (Ogata, 2001), in which a process output variable (r(t)) is compared to a reference setpoint (r(t)), establishing the instantaneous error (u(t)) and generating a correction signal from to the PID (u(t)). This general process is depicted in Fig. 2.

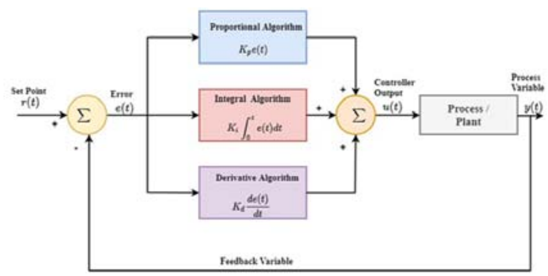

Figure 2. Classic layout of a PID controller (Borase et al., 2021).

The PID controller output signal u(t) is dependent on the proportional, integrative and derivative gains K_p, K_I and K_d respectively. These values are adjustable and defining them is the subject of study of several well-established technical publications. One of the most recognised techniques was proposed by Ziegler and Nichols (Ogata, 2001), wherein the integrative and derivative gain values are zeroed while the proportional gain is increased up to an instability threshold. Similarly, CHR (Daful, 2018) and Tavakoli (Tavakoli and Tavakoli, 2003) methods are based on minimising the error through fine tuning each gain component, with satisfactory results and widespread industry implementation, albeit the relatively long and complex intermediate calculation processes.

The recent advances in Artificial intelligence have enabled the proposition of machine learning techniques to predict and set optimal values for the gains in a PID under a wide range of operating requirements. This way, the conventional labour-intensive heuristic methods can be replaced by AI techniques, allowing for faster and more precise control PID operation. In the present work, the PID control setpoint will be used as reference to train and supervise the ANN, with the latter response used to tune the K_p , K_I and K_d to reach a satisfactory error and overall operation.

ARTIFICIAL NEURAL NETWORK

Artificial Neural Networks mimic the biological neuron learning process, by adjusting weights that define their output magnitude. In actual neurons, these weights are chemicals that enhance or inhibit synaptic information transmission, and once a task is successfully executed, the optimal chemical concentration information is stored for when the action is repeated (Nunes et al., 2010).

In this work three feedforward Multilayer Percepton (MLP) ANN, integrated to an automotive air conditioning PID controller was proposed to define and tune its proportional, integrative and derivative gains, as schematically depicted in Fig. 3.

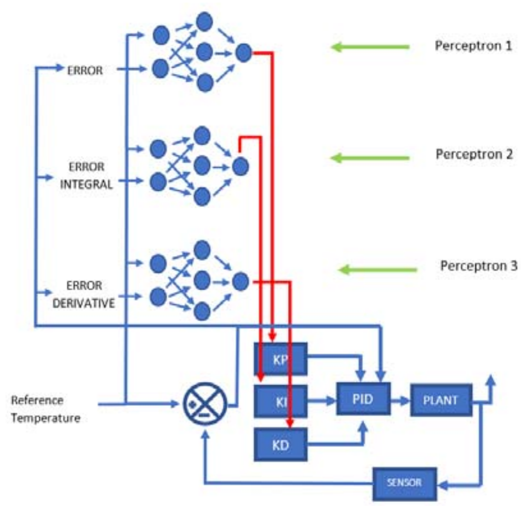

Figure 3. Integration layout of the artificial neural network with the PID controller.

Functional description of a Perceptron ANN (Ramchoun et al., 2016) will now be provided, in the following Fig. 4. In this figure, the proposed ANN topology consists of an input layer, wherein the process measured variables enter, an intermediate hidden layer and the output layer, responsible for setting the PID controller gain values. Data entering the ANN through the input layer is distributed to all neural nodes in the intermediate layer, where a set of mathematical relations are applied before transferring the information to the output node, corresponding to the instantaneous optimal gain.

The data processed by each hidden layer neural node (J_n) is defined as the product between the previous neuron data (i_n) and a weighting factor (x_{ij}), decreased by an activation function (θ)

$$J_n = \sum_1^n (i_n \cdot x_{ij} - \theta) \tag{7}$$

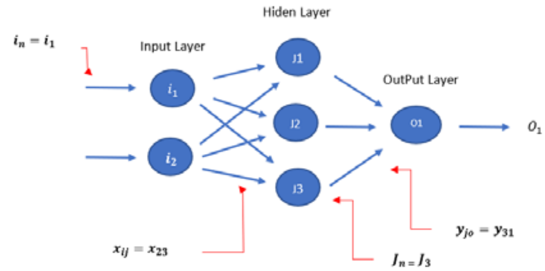

Figure 4. Integration layout of the artificial neural network with the PID controller.

Similarly, the output layer processed data is given by the product between the hidden layer processed data (J_n) and the weighting factor y_{jo}, decreased by the activation function θ

$$O_1 = \sum_1^n (J_n \cdot y_{jo} - \theta) \tag{8}$$

Each hidden layer neural node inlet signal -s- passes through an activation function f(s), comparing it with an activation limit threshold. Several activation function models have been proposed and studied in publications, namely the Sigmoid (or logistic) Activation Function as it is bounded and differentiable, and thus, allowing its use in Back Propagation learning routines (Mudia, 2020). It is expressed as an inverse exponential,

$$f(s) = \frac{1}{1 + e^{-\beta \cdot s}} \tag{9}$$

In which β is a real constant associated with the sigmoid function slope. Regarding the proposed perceptron ANN supervised learning, each neural node signal output is compared to a desired reference, and the absolute deviation magnitude between these values dictates the synaptic weights correction. For instance, if the node output deviates from the desired response, the synaptic weight and activation threshold are increased accordingly to compensate. This convergence process is repeated for each available training sample, resulting in sets of synaptic weights and activation functions that better fit the desired response. This iterative learning process can be mathematically represented by

$$W_i^k = W_i^{k-1} + \eta \cdot (d^k - y) \cdot \delta \cdot x^k \tag{10}$$

$$\theta_i^k = \theta_i^{k-1} + \eta \cdot (d^k - y) \cdot \delta \cdot x^k \tag{11}$$

Where η is a constant defined by the ANN learning rate, y is the perceptron instantaneous outlet signal, d^k is the known desired response for the k^{th}

training sample, δ is the gradient and, lastly, W is the weights vector. The proposed three-layer perceptron ANN supervised learning (Eqs. (10) and (11)) is limited to the output layer. The hidden layer weight and activation thresholds are defined by a backpropagation learning technique, which calculates the magnitude error of the outlet layer compared to the supervised training sample data through the equation:

$$E(k) = \frac{1}{2} \cdot \sum_{j=1}^{n} (d_j^k - y_j^k)^2 \tag{12}$$

Applying the derivative chain rule, it is possible to conclude the weight matrix W must be updated in the opposite direction to the error propagation, aiming thus to minimise the latter. This means the updated weight matrix W^k will be equal to its previous step value W^{k-1} added to a compensating correction, resulting in minimum error $E(k)_{min}$. A noteworthy distinction between the hidden and output layer is that the former does not have an user input reference value to compare to, and depends on the output layer signal error feedback to adjust its synaptic weights and activation (hence the Backpropagation nomenclature). Through training iterations of this process, weights and limits of each intermediate node within the hidden layer are adjusted and updated, resulting in a set of values that best correlates the known reference data with the given input signal.

SIMULATION

Firstly, it is important to describe how the ANN set the controller gain components: (i) Perceptron 1 ANN (see Fig. 3) was trained by comparing the absolute magnitude of the PID controller error with the set temperature reference, with its output layer signal used to define the controller proportional gain K_p; (ii) Perceptron 2 has been trained through the integral of the error with respect to the temperature setpoint, with its output layer returning the integral gain value K_I; (iii) Perceptron 3 has been neglected in the simulation since this practice is common for process with fast changes on the manipulated variable. The training data used by the network are shown in Tab. 1.

During the supervised training stage, values for the PI proportional and integrative gains were defined using conventional Ziegler Nichols methods, whereas the ANN learning was performed through Matlab's Neural Net Fitting tool (nftool) (Ballabio and Vasighi, 2012). This function emplys a sigmoidal activation (Eq. (9)) with a linear output layer, as depicted in Fig. 5.

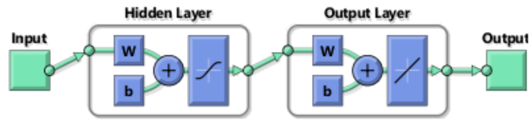

Figure 5. Layout of the nftool neural network.

The reference thermal load utilised as the reference desired output data was extracted from (Marcos et al. 2014), consisting on a commercial vehicle exposed to ambient sunlight, but without passengers. In these conditions, the reference paper described a linear response between the thermal load and passenger compartment, Eq. (13)

$$\dot{Q} = \frac{T}{0.0601} \tag{13}$$

Combining Eqs. (13) and (6), the required refrigerant mass flow rate through the air conditioning system that attends to the thermal requirement is:

$$\dot{m}_f = \frac{\frac{T}{0.0601}}{c_{pf} \cdot (T_{in} - T_{out})} \tag{14}$$

In the reference paper (Marcos et al. 2014), the studied refrigerant was R134a. Its flow rate control is achieved on a throttle valve, where it leaves with vapour quality equal to null. In the evaporator unit, which follows the metering device, the R134a enters at 250K (-23,15ºC) and undergoes a temperature increase equal to 5K (Rajamanickam and Tamilselvan, 2017). This knowledge allows for Eq. (15) to be written to determine the required mas flow rate as a linear temperature function,

$$\dot{m}_f = 2.59 \cdot 10^{-3} \cdot T \tag{15}$$

Or, solving for the differential form

$$386.10 \cdot \frac{dm}{dt} = T \tag{16}$$

This alternative formulation allows for Laplace transform to be applied, converting the time-domain function f(t) to a complex frequency response F(s)

$$386.10 \cdot s \cdot Y(s) = U(s) \tag{17}$$

$$\frac{Y(s)}{U(s)} = G(s) = 2.59 \cdot 10^{-3} \cdot \frac{1}{s} \tag{18}$$

Table 1. Data used for the network training

$\dot{m}_f$	ABSOLUTE ERROR	ERROR INTEGRAL	K_P	K_I
0.03885	-0.0000011610	0.00003370	96.03	4.440
0.04144	0.0000223900	0.00000500	95.50	4.393
0.04403	-0.000002256	0.00005686	91.71	4.049
0.04662	-6,94E-15	3,98E-13	88.68	3.805
0.04921	-0.000000600	0.00002181	92.85	4.146
0.05180	-6,37E-07	2,56E-05	92.61	4.146
0.05439	-0.000002786	0.00007024	91.71	4.049
0.05698	0.000030790	0.00010290	95.50	4.393
0.05957	0.000001978	-0.00001969	96.01	4.388
0.06216	0.000005800	0.00018810	100.3	4.768
0.06475	0.000002170	0.00017780	100.5	4.811
0.06734	0.000001275	0.00017620	99.14	4.664
0.06993	0.000009672	0.00003889	99.51	4.713
0.07252	0.000002309	0.00027720	100.0	4.817
0.07511	0.000007928	0.000012520	111.2	5.932
0.07770	0.000007249	0.000005245	100.3	4.768

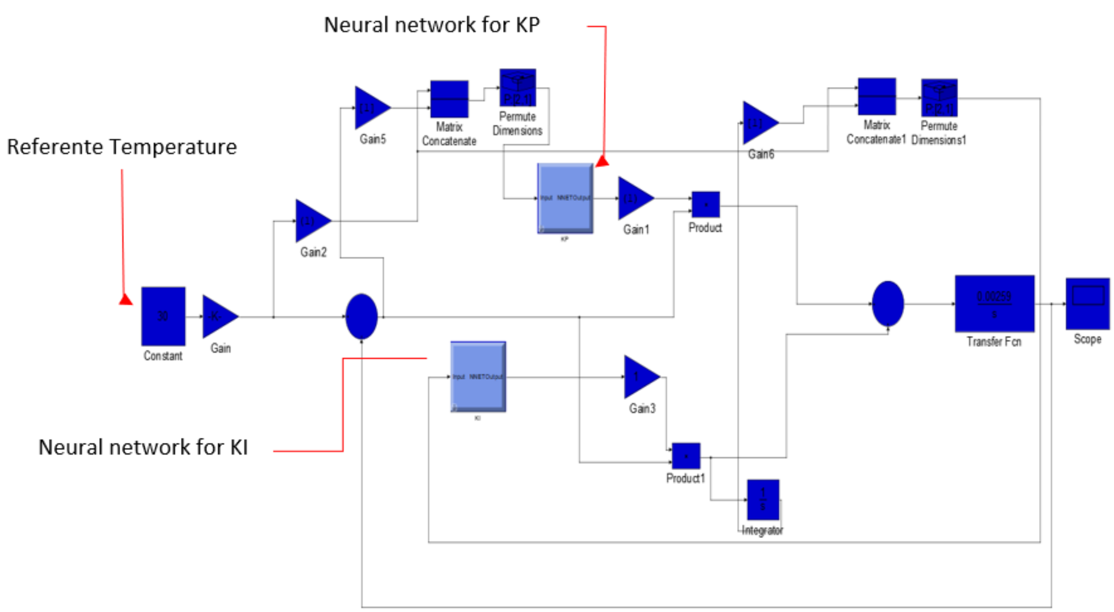

Figure 6. Neural PI– SIMULINK.

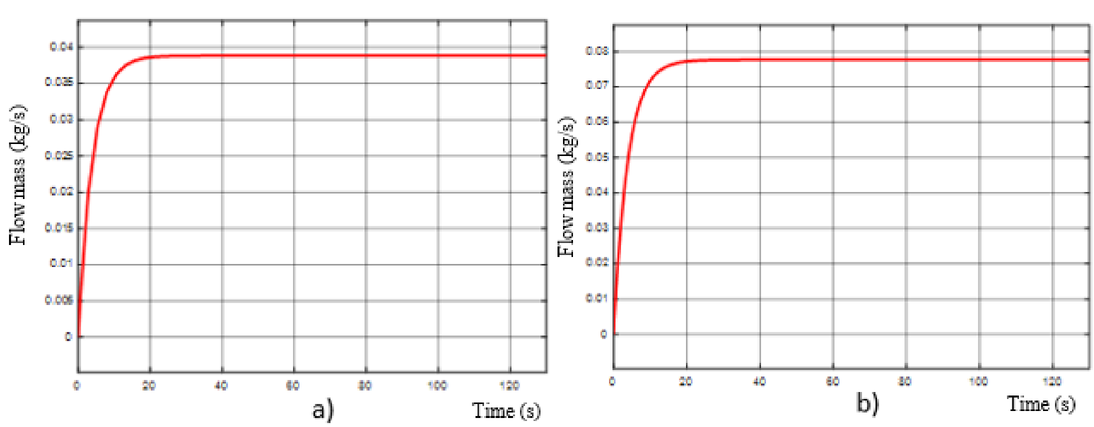

Figure 7. Response for a) Tref =15ºC e b) Tref=30ºC.

Matlab's Simulink interface was used to simulate the ANN, PI controller and Laplace transfer function, as depicted in Fig. 6.

RESULTS AND DISCUSSION

The proposed ANN-controller setup, shown in Fig. 6 was tested under setpoints varying between 288 to 308 K (15-35°C). The system control response time has been significantly decreased through implementation of an Artificial Neural network tuning method when compared to conventional manual alternatives. The system time of response on the upper and lower temperature limits are shown in Fig. 7(a) and Fig. 7(b).

The stabilisation response time slightly increases as the setpoint temperature rises. When the reference temperature equals 15°C, the elapsed time before stabilisation is 35.2s, while at 35°C it took 39 seconds. This behaviour is shown in Fig. 8.

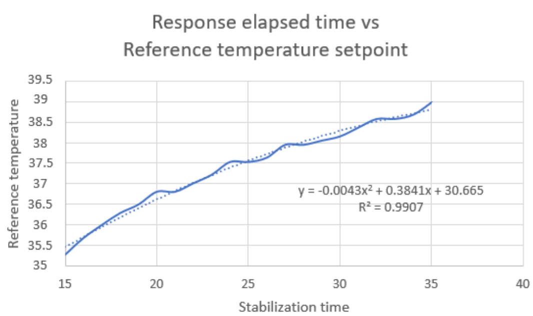

Figure 8. Response elapsed time by reference temperature.

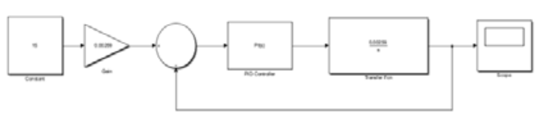

Figure 9. PI Controller without Artificial Neural Network – Ziegler Manual tuning Nichols.

In this manual tuning setup, the required stabilisation time increased so significantly it cannot be considered to practically reach stable response. The elapsed time, not considering the actual gain tuning, figured at around 4000 s (over one hour). This exposes the importance of proper tuning in the system response time.

CONCLUSIONS

Keeping in mind the escalating importance of performance optimisation on automotive air conditioning systems, especially due to recent environmental concerns, the present work proposed an innovative Artificial Neural Network (ANN) – PID control system integration, in which the integrative, derivative and proportional gain components would be continuously monitored and adjusted aiming to minimise the system response time. A thermal model was set up, and shown that the system refrigerant mass flow rate is directly proportional to the net thermal load. Following, the PID controller model operation and integration with ANN have been thoroughly presented. The ANN in question consists on an optimised, training supervised multi-layer Perceptron responsible for defining the PID controller gain values. In the specific case, the derivative component can be disregarded, due to the passenger compartment temperature rapid changing nature.

Matlab's Simulink was the chosen interface to simulate the automotive air conditioning system, with boundary conditions determined by literature references under similar operating conditions. The differential equation resultant from the thermal is the input for a Laplace transform, allowing for its implementation into the PI tuning process. Two ANN's neurons have been set, responsible for calculating the respective PI gain component. Each consists of a six-node sigmoidal hidden layer, single-node linear response output layer. The first neuron was responsible for the proportional gain definition, by comparing the instantaneous error magnitude to the reference temperature while the second calculated the integrative gain component through the error integral. During the supervised training period, the desired gains were calculated through Ziegler Nichols methods, reaching R^2 values equal to 0.9012 and 0.9668 for the first and second neurons, respectively.

To compare the improvements achieved by the ANN-PI controller, two similar setups were simulated. The first utilised classical methods to determine integrative and proportional gains, while the second implemented the aforementioned described ANN. Simulation results have shown the significant response improvement, with the novel integrated proposition taking around half minute to stabilise whilst the conventional solution required over one hour to achieve similar results. Not only the response time decreased, but also the overall operation is simplified by the ANN automatically determining the optimal gain values without requiring manual interventions.

Overall, implementing an Artificial Neural Network to an automotive air conditioning control system resulted in satisfactory performance gain, and ultimately, allows for higher fuel efficiency.

REFERENCES

Ballabio, D., and Vasighi, M., 2012, A MATLAB Toolbox for Self Organizing Maps and Supervised Neural Network Learning Strategies, Chemometrics and Intelligent Laboratory Systems, Vol. 118, pp. 24–32. https://doi.org/10.1016/j.chemolab.2012.07.005.

Borase, R. P., Maghade, D. K., Sondkar, S. Y., and Pawar, S. N., 2021, A Review of PID Control, Tuning Methods and Applications, International Journal of Dynamics and Control, Vol. 9, pp. 818-827. https://doi.org/10.1007/s40435-020-00665-4.

Daful, A. G., 2018, Comparative Study of PID Tuning Methods for Processes with Large & Small Delay Times, in: *2018 Advances in Science and Engineering Technology International Conferences, ASET*, United Arab Emirates, pp. 1-7. https://doi.org/10.1109/ICASET.2018.8376915.

European Commission, 2006, Directive 2006/40/EC of the European Parliament and of the Council of 17 May 2006 Relating to Emissions from Air-Conditioning Systems in Motor Vehicles and Amending Council Directive 70/156/EEC, Official Journal of the European Union, 161, 12–18.

Fayazbakhsh, M. A., and Bahrami, M., 2013, Comprehensive Modeling of Vehicle Air Conditioning Loads Using Heat Balance Method, in: *SAE 2013 World Congress & Exhibition,* Technical Papers 2013-01-1507. https://doi.org/10.4271/2013-01-1507.

Hassan, H., 2013, Kyoto Protocol: One step in 1K mile way. Retrieved April 17, 2021, from https://www.researchgate.net/publication/236347433_Kyoto_Protocol_paper-mod.

Khayyam, H., Kouzani, A. Z., and Hu, E. J., 2009, Reducing Energy Consumption of Vehicle Air Conditioning System by an Energy Management System, in: *2009 IEEE Intelligent Vehicles Symposium*, Xi'an, pp. 752–57. https://doi.org/10.1109 / IVS.2009.5164371.

Marcos, D., Pino, F. J., Bordons, C., and Guerra, J. J., 2014, The Development and Validation of a Thermal Model for the Cabin of a Vehicle, Applied Thermal Engineering, Vol. 66, No. 1–2, pp. 646–656. https://doi.org/10.1016/j.applthermaleng.2014.02.054.

Mudia, H., 2020, Back Propagation Neural Network for Controlling Coupled Water Tank, Bulletin of Computer Science and Electrical Engineering, Vol. 1, No. 1, pp. 12-18.

Nie, L., Guan, J., Lu, C., Zheng, H., and Yin, Z., 2018, Longitudinal Speed Control of Autonomous Vehicle Based on a Self-Adaptive PID of Radial Basis Function Neural Network, IET Intelligent Transport Systems, Vol. 12, No. 6, pp. 485–494. https://doi.org/10.1049/iet-its.2016.0293.

Nunes,I., Hernane,D., and Andrade, R., 2010, *Redes Neurais Artificiais Para Engenharia e Ciências Aplicadas*, Artliber.

Ogata, K., 2001, *Modern Control Engineering*, Prentice-Hall, 4 Edition.

Rajamanickam, C. S., and Tamilselvan., P., 2017, Multiphase Simulation of Automotive HVAC Evaporator Using R134a and R1234yf Refrigerants, International Journal of Mechanical Engineering and Technology, Vol. 8, No. 2, pp. 263–70.

Ramchoun, H., Ghanou, Y., Ettaouil, M., and Idrissi, M. A. J., 2016, Multilayer Perceptron: Architecture Optimization and Training, International Journal of Interactive Multimedia and Artificial Intelligence, Vol. 4, No. 1, pp. 26-30. https://doi.org/10.9781/ijimai.2016.415.

Sen, R., Chinmoy, P., Samik. D., and Ranjan, S., 2014, Comparison Between Three Tuning Methods of PID Control for High Precision Positioning Stage, Mapan - Journal of Metrology Society of India, Vol. 30, No. 1, pp. 65–70. https://doi.org/10.1007/s12647-014-0123-z.

Tavakoli, S., and Tavakoli, M., 2003, Optimal Tuning of PID Controllers for First Order Plus Time Delay Models Using Dimensional Analysis, in: *4th International Conference on Control and Automation Proceedings*, Montreal, pp. 10-12. https://doi.org/10.1109/ICCA.2003.1595161.

Visioli, A., 2001, Tuning of PID Controllers with Fuzzy Logic, IEE Proceedings: Control Theory and Applications, Vol. 148, No. 1, pp. 1–8. https://doi.org/10.1049/ip-cta:20010232.

Yang, C. Y., and Hamid, N., 2018, Condensation Heat Transfer and Pressure Drop of Refrigerants HFO-1234yf and HFC-134a in Small Circular Tube, International Journal of Heat and Mass Transfer, Vol. 127, pp. 218–27. https://doi.org/10.1016/j.ijheatmasstransfer.2018.07.093.

Zhang, D., Muhammad, A. A., Zhenling, L., Wan, X. P., Mohammad, J. G., and Amirhosein, M., 2020, Dynamic Modeling and Adaptive Controlling in GPS-Intelligent Buoy (GIB) Systems Based on Neural-Fuzzy Networks, Ad Hoc Networks, Vol. 103, No. 1, pp. 1–11. https://doi.org/10.1016/j.adhoc.2020.102149.